

Looking for active faults at east Qattara depression, northwestern desert, Egypt

Taha Rabeh*

Received: April 01, 2011; accepted: February 07, 2012; published on line: September 28, 2012

Resumen

Los datos del campo potencial son considerados el principal factor que sustenta los procesos de exploración geofísica, utilizados para detectar y evaluar las estructuras del subsuelo. En este caso se realizó en el campo una recopilación detallada de datos magnéticos en el área escogida anteriormente para la investigación sísmica. El objetivo principal de este estudio, es detectar las estructuras más profundas del subsuelo y investigar las posibles relaciones de estas estructuras con la actividad sísmica.

El mapa de RTP aeromagnéticos fue usado para detectar la extensión regional de las estructuras de interpretación a partir del trabajo de prospección magnética. Las interpretaciones fueron realizadas en mapas RTP del terreno y aeromagnéticos utilizando, técnica de filtrado, separaciones del mínimos cuadrados, análisis de tendencias tectónicas, análisis espectral, el método de Werner, y Euler y dos técnicas de dimensiones. Los resultados muestran que las principales tendencias tectónicas dominantes son N35° - 45°W, N45°- 65° E, E -W y las tendencias de Aqaba.

Por otra parte WQ85 dos líneas sísmicas-31B y 127 fueron interpretados y la localización de estas líneas son coincidentes con el mapa tectónico deducido. Los resultados muestran que existe una gran coincidencia entre la ubicación de las fallas deducidas de los datos geomagnéticos y sísmicos. Los resultados obtenidos indican una buena relación con los datos de pozos.

Además, estas estructuras están relacionadas con las actividades del terremoto registrado por el National Egyptian Seismological Network (ENSN). La correlación permite deducir que la zona de estudio es más estable que otras áreas adyacentes en el norte de Egipto, cerca del mar Mediterráneo y el río Nilo Delta.

Palabras clave: prospección magnética, líneas sísmicas, estructuras del subsuelo.

Abstract

Potential field methods are considered the cheapest tools in geophysical exploration to detect and characterize subsurface structures. Here we present a detailed land magnetic survey in an East Qattara Depression that was subjected before to a reflection seismic investigation. The main target of this study is infer the deeper subsurface structures and to investigate possible relations of these structures with earthquake activity.

The reduced to north Pole (RTP) aeromagnetic map was used for detecting the regional extension of the interpreted structures on the land magnetic survey. The interpretations were performed on the RTP land and aeromagnetic maps using filtering techniques, least squares separations, tectonic trend analysis, spectral analysis, Werner and Euler deconvolutions, and 2.5-D modelling techniques. The results indicate that the main dominant tectonic trends are N35°- 45°W, N45°-65°E, E-W and Aqaba trends.

Moreover two seismic lines WQ85-31B and 127 were interpreted and compared with the deduced tectonic map. The results show that there is a great correlation between the location of the faults deduced from both the magnetic and seismic data. The results agree with the well logging data.

Furthermore these structures correlated with the recorded earthquake activity by the National Egyptian Seismological Network (ENSN). This correlation implies that the studied area is more stable than other adjacent areas in the northern parts of Egypt close to the Mediterranean Sea and the Nile Delta River.

Key words: magnetic survey, seismic lines, subsurface structures.

T. Rabeh*
National Research Institute of Astronomy
and Geophysics Helwan

Cairo, Egypt and IDL, Lisbon, Portugal

*Corresponding author: taharabeh@yahoo.com

Introduction

The study area lies between $29^{\circ} 50'$ and $30^{\circ} 25'$ of Latitude N and $28^{\circ} 15'$ and $28^{\circ} 50'$ of Longitude E, at the eastern part of Qattara Depression of the North Western Desert (Figure 1), covering an area of about $1,000 \text{ km}^2$. Seismic reflection studies have been done in this area by many petroleum companies including Khalda Petroleum Co. (2000), and Badr El Din Petroleum Co. (2004) which are considered the largest oil companies with concessions in the study area.

An comprehensive land magnetic survey in a mesh like form was conducted also. The distances between the stations range between 200 to 500 m depending on the topography obstacles and rate of the magnetic field variations. The magnetic data were corrected by diurnal and latitude variations and finally reduced to the north magnetic Pole. The RTP magnetic maps were subjected to qualitative analysis using trend analysis, and two dimensional wavelength filtering techniques (Zurflueh, 1967).

Also, quantitative interpretation was performed along profiles crossing the studied area from east to west and from north to south, using spectral analysis and 2.5 - D magnetic modelling techniques using commercial software (GM-SYS, 1995).

2.5-D magnetic profiles were selected along two seismic lines (line WQ85-51B and line 127). A good correlation is observed between the features of the seismic lines and the features on the structural maps obtained from the magnetic data, and the 2.5-D magnetic modelled profiles.

Geology and tectonic setting of the area

The study area, as part of North Western Desert region, its geology bears the common following regional features. The stratigraphic sequence overlying the basement complex in the North Western Desert generally comprises three major lithological divisions as proposed by Said (1990), Barakat (1982) and Abdel Hady *et al.* (1988). From base to top we have (i) Lower Clastic Division of Pre-Cenomanian age, (ii)

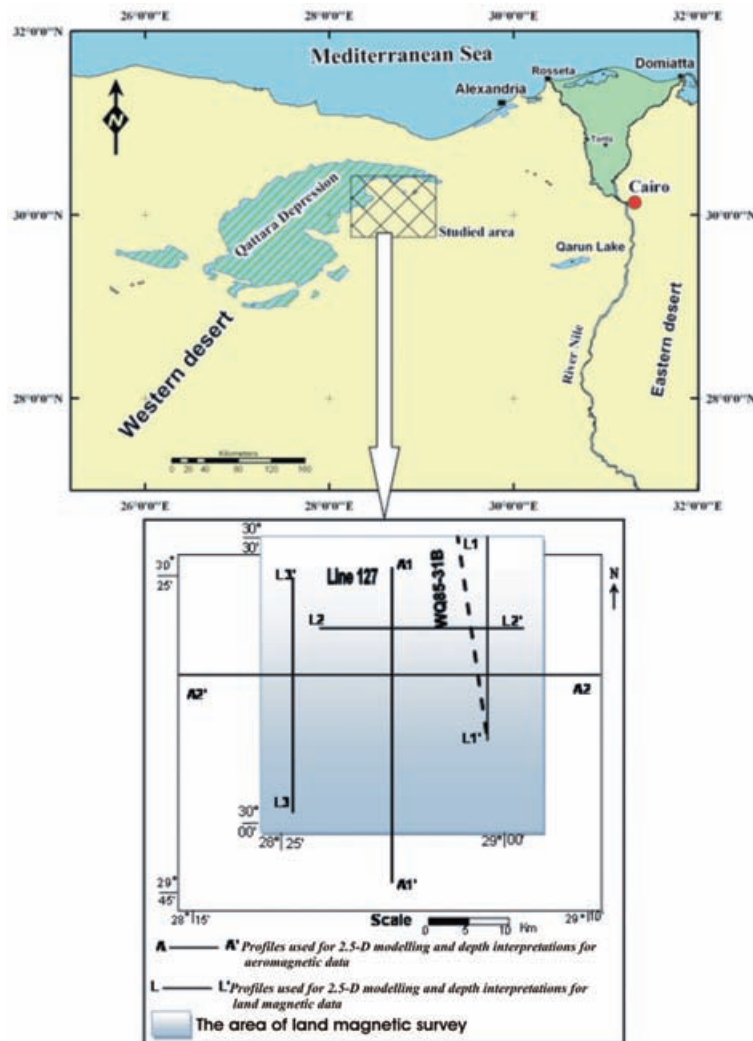


Figure 1. Location map of the study area showing the profiles used for seismic and magnetic interpretations.

Middle Calcareous Division of Cenomanian to late Eocene age (iii), and the Upper Clastic Division of Oligocene to recent age.

The surface geology (Figure 2) of the studied area shows that more than 80% of the zones covered by limestones of Miocene age is constituted by Sabkhas (evaporite-carbonate) deposits in the middle part. Sandstones and other Quaternary deposits with some minor Oligocene rocks are occupying the north-eastern part of the study area.

Recent seismicity mapped by Egyptian National Seismological Network (1997-2003) (Figure 3) indicates that the study area is featured a very low seismic activity, and earthquake activity is almost missing. This explains in part why surface faults (Figure 3) are absent or rare. This indicates also that the recent tectonics of the study area are more stable than others adjacent areas close to the Mediterranean sea or Nile-Delta.

Data acquisition and interpretation

A detailed land magnetic survey was made in the study area using two Proton magnetometers. One of them was fixed at the selected base

station, while the other was used to measure the total intensity along the stations that cover the study area in a mesh like form. The measured data were corrected for diurnal variations and for latitudes towards the north.

These data were digitized by computer digitizing programs and the total magnetic anomaly map was obtained. This map was reduced to the North Magnetic Pole using suitable FORTRAN program after Baranov (1975) (Figure 4). The RTP map illustrates the exact positions of the magnetic anomalies distributed all over the studied area. Furthermore, a RTP aeromagnetic anomaly map (Figure 5), was also used in the interpretation to illustrate the regional extensions of the subsurface structures.

The RTP magnetic maps indicate that most of these anomalies are aligned in NW-SE, NE-SW, and E-W directions. The deepest anomalies sources in the NE and SW portions as indicated by the presence of negative anomalies that imply thick sedimentary sequences, and from correlated drilled wells in these parts. The shallowest parts extend from NW to SE direction as indicated by the presence of positive anomalies and data from the drilled wells.

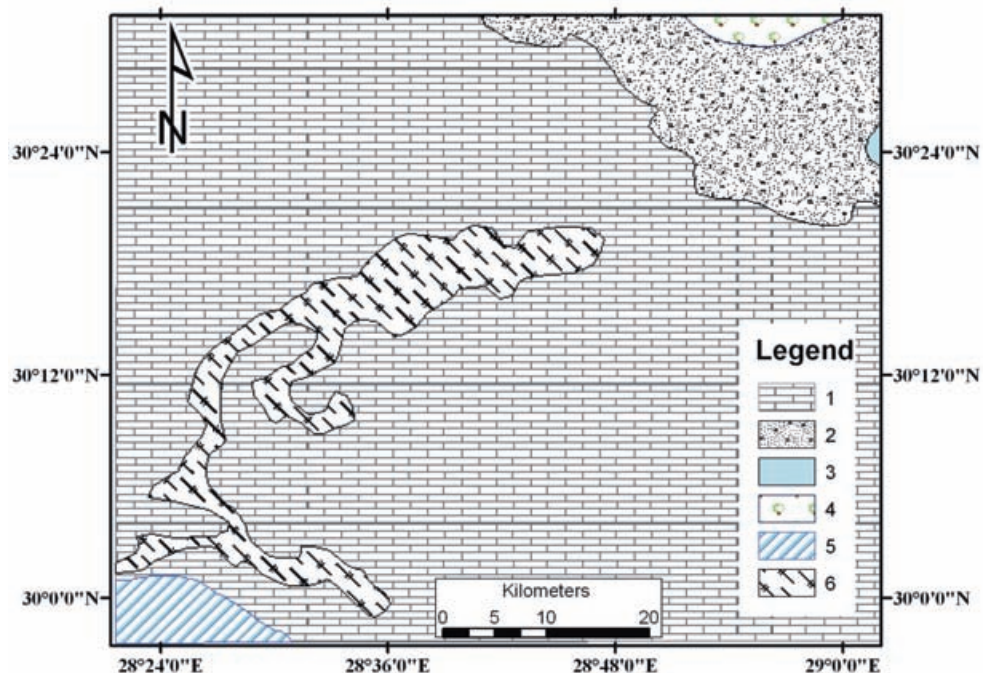


Figure 2. Surface geologic map of the study area after CONOCO (1987). 1- Miocene limestone, 2- Quaternary deposits, 3- Oligocene rocks, 4- Sand dunes, 5- Eocene limestone, 6- Sabkhas deposits.

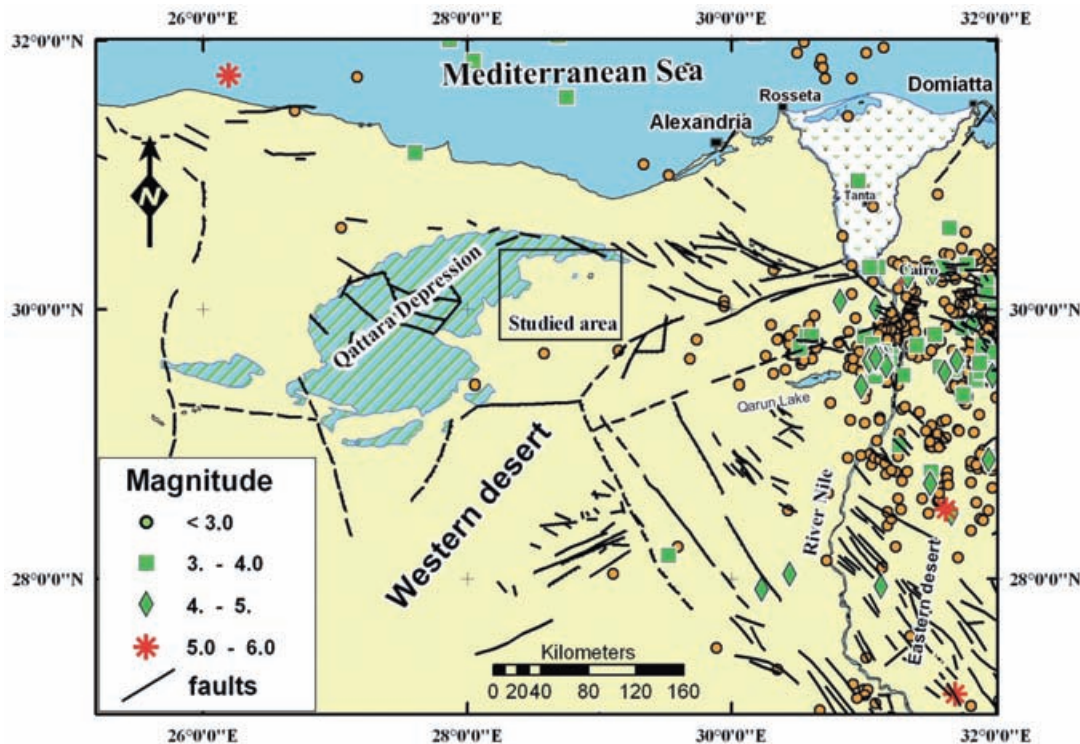


Figure 3. Recent earthquakes activity (1997- 2003) in the north western part of Egypt. Earthquake data were recorded by Egyptian National Seismological Network (ENSN).

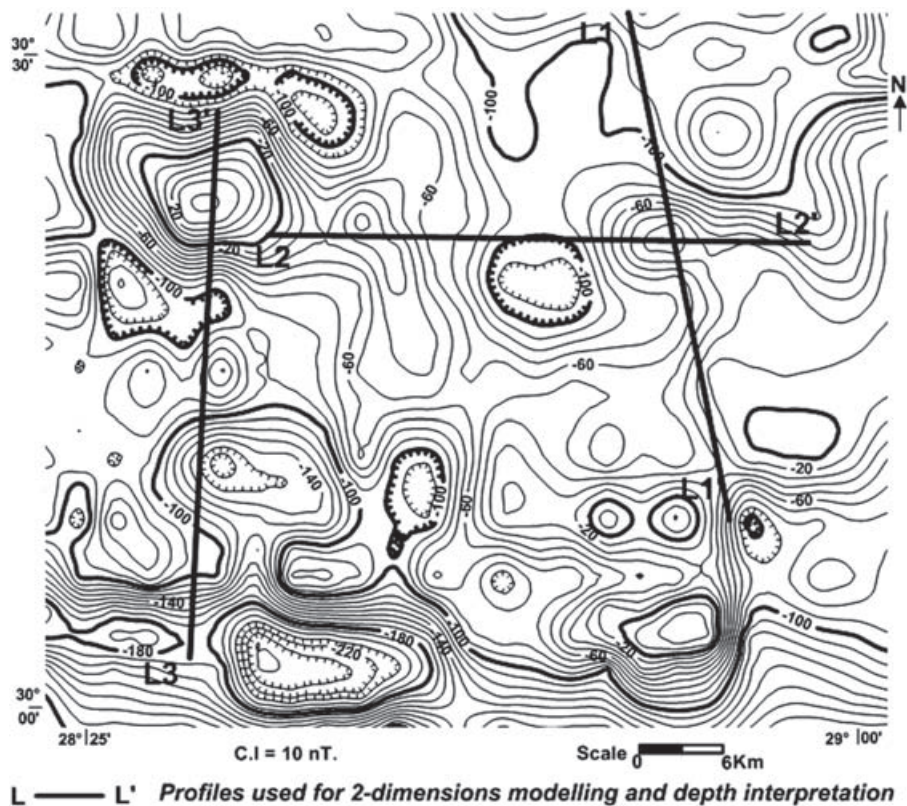
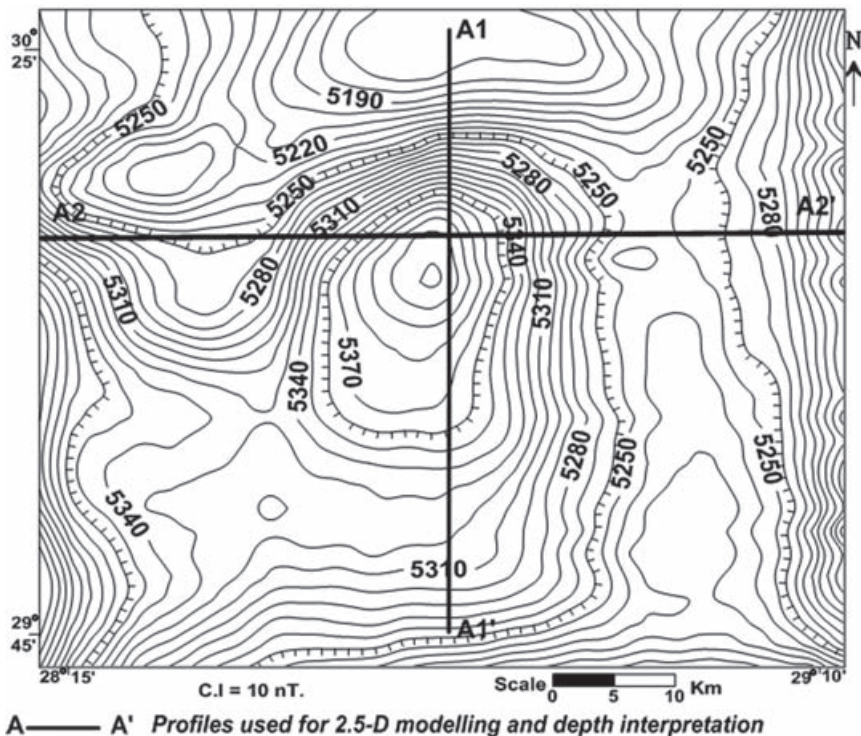


Figure 4. RTP land magnetic map of study area.

Figure 5. RTP aero-magnetic anomaly map of the study area after Egyptian General Petroleum Cooperation (1979).



Filtering technique

Wavelength linear filtering was applied to the RTP magnetic anomaly map. Fourier transform (Hildenbrand, 1983) processing was performed using three types of filters: (1) Low-cut of the residual anomalies with short wavelengths, high frequencies and shallow depths, (2) High-cut of the regional anomalies with long wavelengths, low frequencies and deep depths and (3) Band-pass of the transitional anomalies with intermediate wavelengths, frequencies and depth ranges.

The obtained maps show that most of the anomalies trend in the NW-SE, NE-SW and NNE-SSW directions. Figures 6 and 7 show regional of the landmagnetic map, and te residual corresponding to the aeromagnetic map.

respectively. It is clear that the negative anomalies at the northeastern and southwestern parts of the studied area are present at different levels. This is could be originated from the presence associated to a thick sedimentary sequence. Meanwhile the positive anomalies extend from the northwest to southeast and could be due to the presence of a thin sedimentary sequence and/or intrusion.

Least squares method

The least square method of Henderson (1960), was applied using Surfer software to the RTP land magnetic and to the RTP aeromagnetic anomaly

maps to the area. First, second, and third order surfaces were fitted to the input magnetic and gravity data. This method consists of fitting a mathematical surface that approximates the regional component of the potential data. In all cases the condition of the least squares solution is $\Sigma R^2 = \text{minimum}$, where R denotes the residuals (Nettleton, 1976). The residual anomaly is given as:

$$RA = \Delta g - Z \quad (1)$$

where Δg is the observed potential data and Z is the regional surface.

The correlation coefficients between successive residual maps were computed in order to determine the optimum order of the regional surface to be used. Results were $r_{21} = 0.854$, $r_{21} = 0.965$, and $r_{34} = 0.546$.

The results indicate that the residual magnetic anomaly maps (Figures 8 and 9) of the second order represent the best fitted maps. Also these fitted maps are more or less analogous to the residual map resulted from the filtered technique.

Trend analysis technique

The RTP maps, together with the filtered maps (residual, band-pass and regional filtered maps) were used to delineate the common structural trends in the studied area. The lengths and trends for each detected lineament on the different maps were measured clockwise from the north.

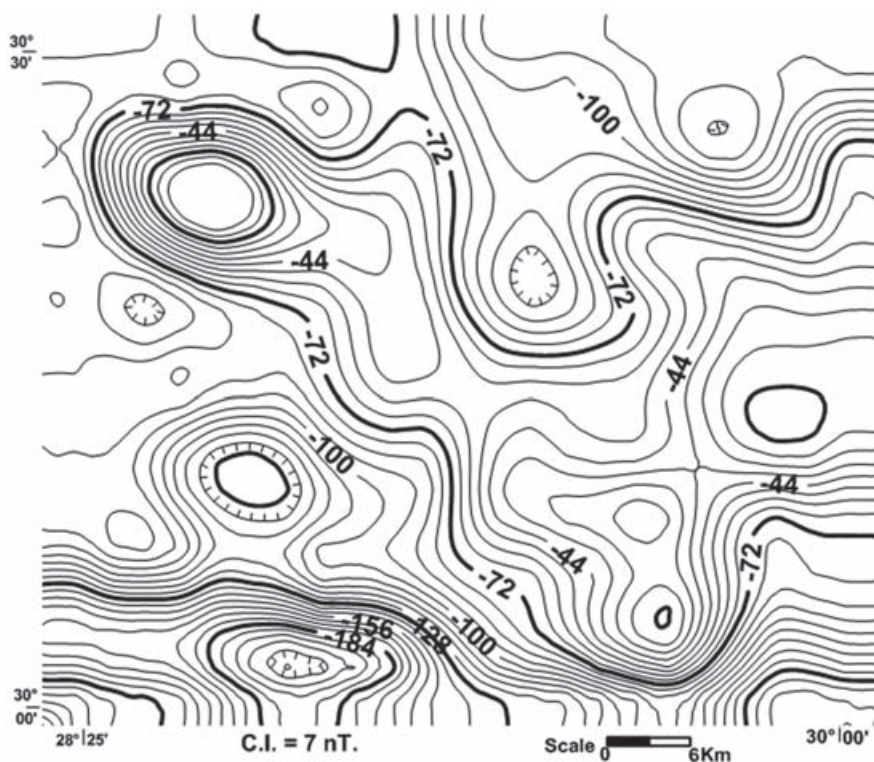


Figure 6. Low-pass regional filtered land magnetic anomaly map.

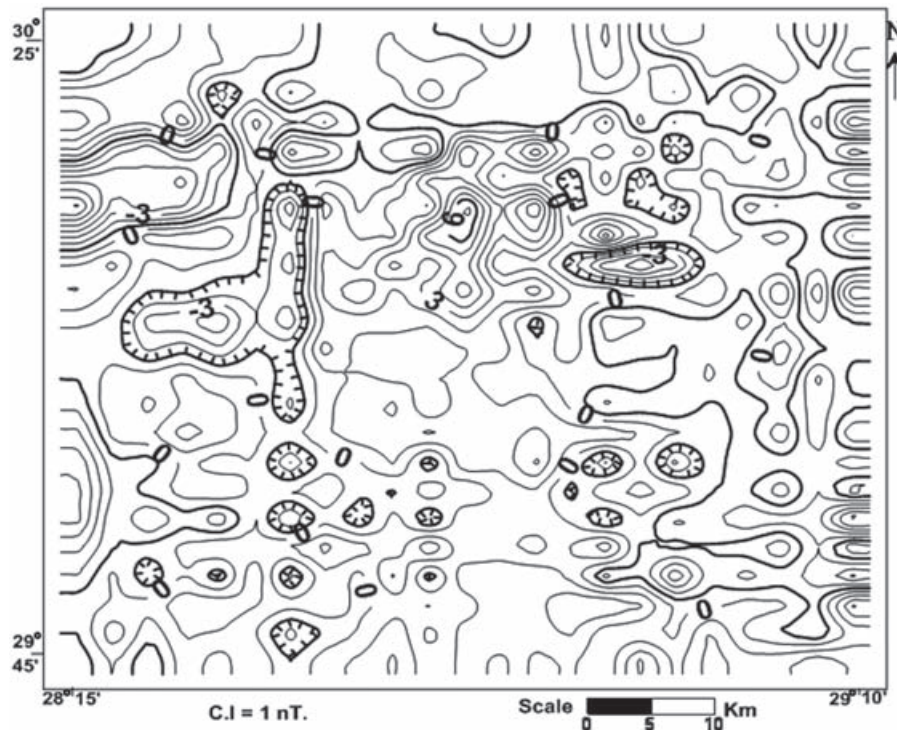


Figure 7. High-pass residual filtered aeromagnetic anomaly map.

Lengths were taken partially in consideration when calculating the statics. The deduced structures map from the land RTP magnetic anomaly map is assumed to represent the fault system affecting the area. On the other hand, the structure maps deduced from the filtered maps

represent faults taking place at different levels (shallow structures deduced from the residual map, intermediate structures deduced from the band-pass filtered map, and deep structures deduced from the regional anomaly map).

Depth estimation methods were applied to the filtered land magnetic maps to determine the mean depth of these structures. In case of Werner deconvolution method the mean values along the basement interface were calculated. Table 1 summarizes the results of Werner deconvolution and spectral analysis methods that would be explained later.

These results confirm that the filtered land magnetic maps represent the distribution of the magnetic anomaly at shallow (mean depth 1 km), intermediate (mean depth 2.3 km) and deep (mean depth 3.6 km) levels respectively.

The deduced fault planes of different directions are grouped every 10° around the north for their length percentage (L %). Statistical procedures have been used to illustrate the predominant

fault trends affecting the studied area. The results of azimuth distribution of both surface and subsurface elements are presented in the form of rose diagrams (Figures 10, 11 and 12).

The results show that the most predominant directions are $N35^\circ - 45^\circ$ W, $N45^\circ - 65^\circ$ E, E - W and Aqaba trends (Figure 11). These trends prevail at the shallow and deep depths lineaments.

Spectral analyses technique

The spectral analysis technique is used for determination of the depth to the basement under the sedimentary cover. This technique depends on the transformation of the space domain into frequency domain by using the Fourier transform.

Table 1. Depth estimation along profiles L1 and L2 of the filtered land magnetic maps.

Regional land magnetic map		Band-pass filtered		Residual land magnetic map		Method / map land magnetic map
Depth in Km		Depth in Km		Depth in Km		
L2	L1	L2	L1	L2	L1	Werner deconvolution method
3.7	3.5	2.25	2.1	1.2	1	
3.5	3.6	2.1	2.31	1.1	1.2	Spectral analysis method

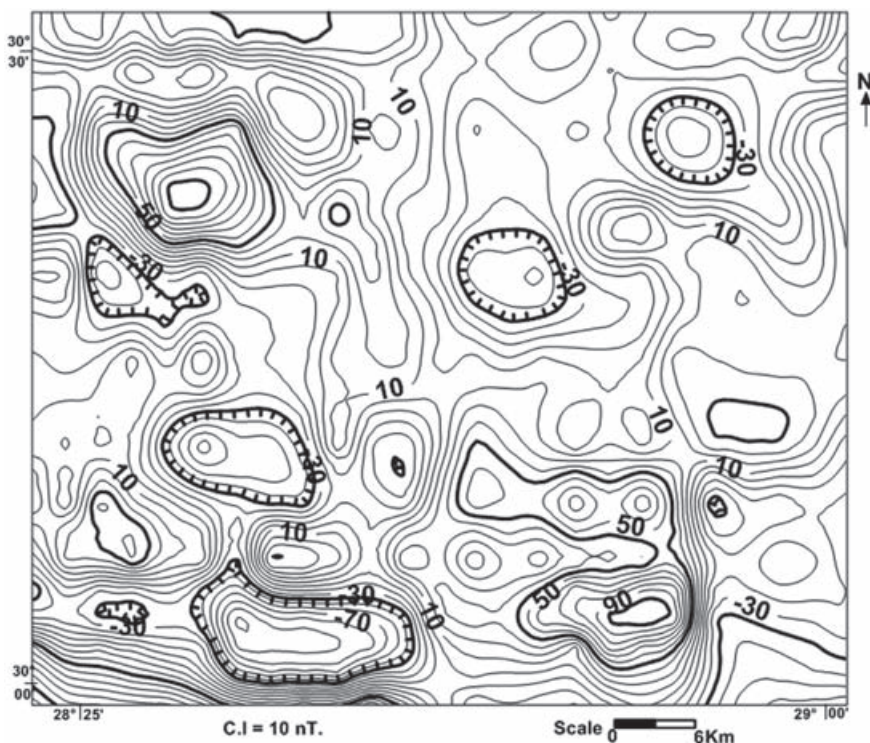


Figure 8. Least square land magnetic map (2nd order) of the study area.

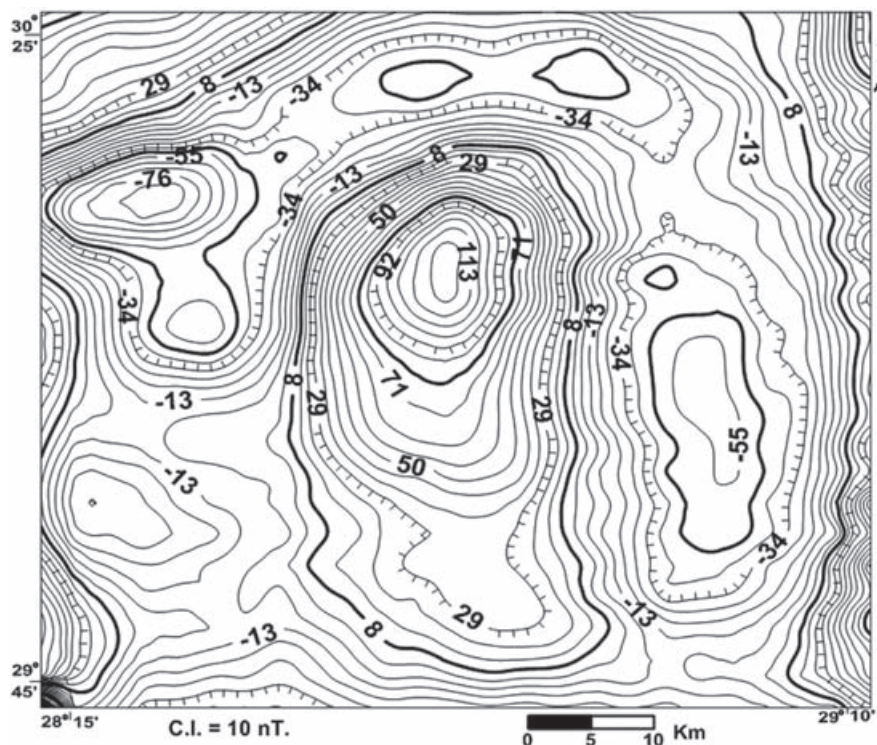


Figure 9. Least square aero-magnetic anomaly map (2nd order) of the study area.

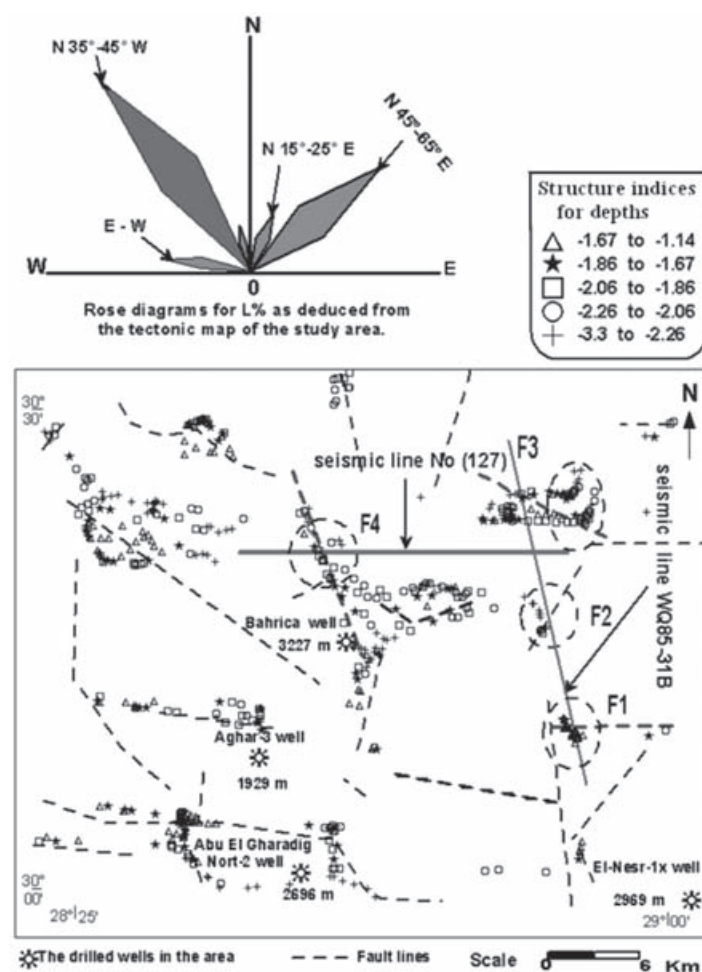


Figure 10. Structure map as deduced from the RTP land magnetic map with location of interpreted seismic lines and the drilled wells in the area.

Figure 11. Structure map as deduced from the RTP aeromagnetic map with location of interpreted seismic lines.

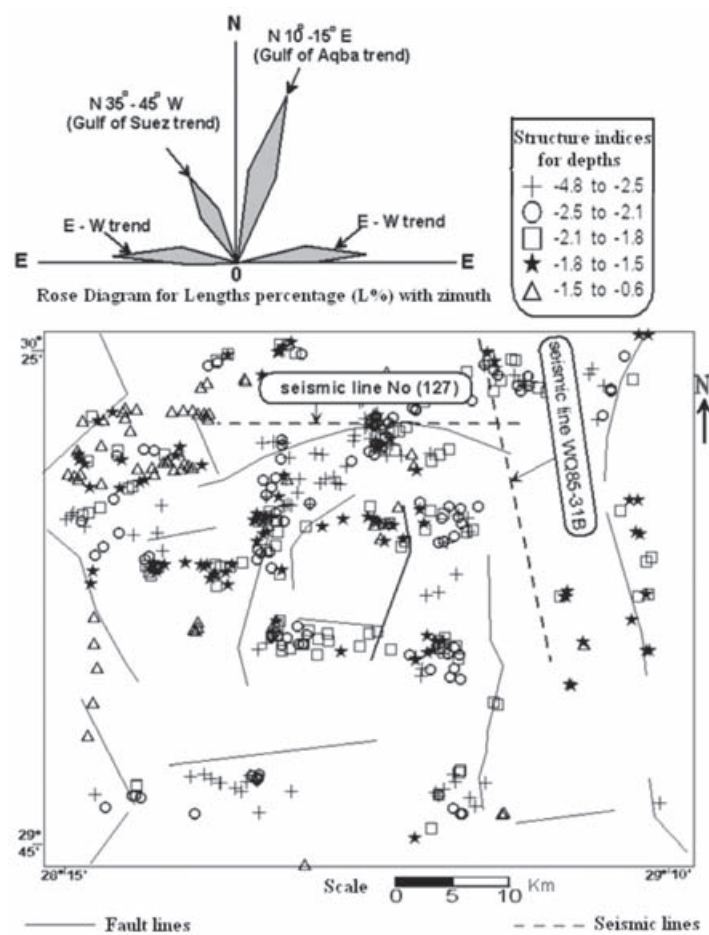
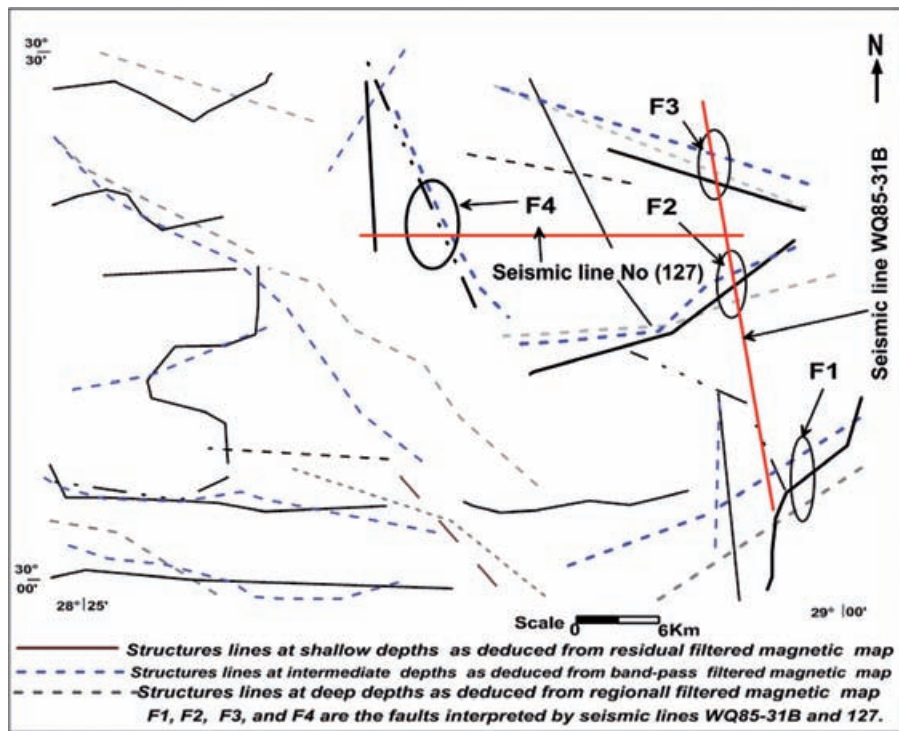


Figure 12. Fault structure lines as deduced from filtered magnetic anomaly maps.



It is expressed mathematically (Båth, 1974) as follows:

$$F(\omega) = \int_{-\infty}^{\infty} f(x) e^{i\omega x} dx \quad (2)$$

where: $F(\omega)$ is the Fourier transform of $f(x)$, $f(x)$ is the value of the function or anomalous potential data at a point x and, ω is the spatial frequency in cycle / unit distance in x . The depth z can be estimated from the graphical diagram of the \ln diagram of the long amplitude spectrum using the relation

$$-z = \tan(\Phi) \quad (3)$$

where: Φ is the dip angle of the straight line approximated in the diagram of the \ln -amplitude spectrum versus the spatial frequency.

The results (Figure 13) show that the main depth increases towards the north and western parts where they reaches volves of about 4.3 km or more and decrease towards the eastern and southern parts where they reaches volves of about 3.5 km. The depth to the intruded rocks ranges between 0.7 to 0.4 km.

Werner deconvolution method

The deconvolution technique (Werner, 1953) is based on the selection of a group of four or more measurements in order to calculate the location of the magnetic body separately. When locations

are plotted in cross sections, the depth estimates tend to cluster around the true location of the causative body. Groups of consecutive points were treated as a "window" sliding along the profile.

The program applied to the RTP geomagnetic data is based on the method developed by Pasteka (2001) aimed to increase and confirm the resulting depths along the selected profiles for horizontal and vertical directions. The results confirm the tectonics deduced from the trend analysis of the RTP geomagnetic maps. Also it illustrates that the mean depth to the basement rocks is ranging between 3.9 and 4.1 km (Figure 14).

Euler deconvolution method

This method has a wide application to determine the subsurface positions (Reid *et al.*, 1990) and the depths to the geomagnetic inhomogeneities. (Thompson, 1982). It is applied to grided data. The method obtains the gradients, locate the square windows within the grids of gradient values and field, and obtain the structural data.

The method was applied to the RTP land magnetic and RTP aeromagnetic grided data using the 0.5 magnetic index, with a window size of 11 km, in order to obtain the depths to the basement rocks and their structures. The results were plotted in X and Y planes (Figures 10 and 11). These results indicate that the depth to the sources reaches about 4 km.

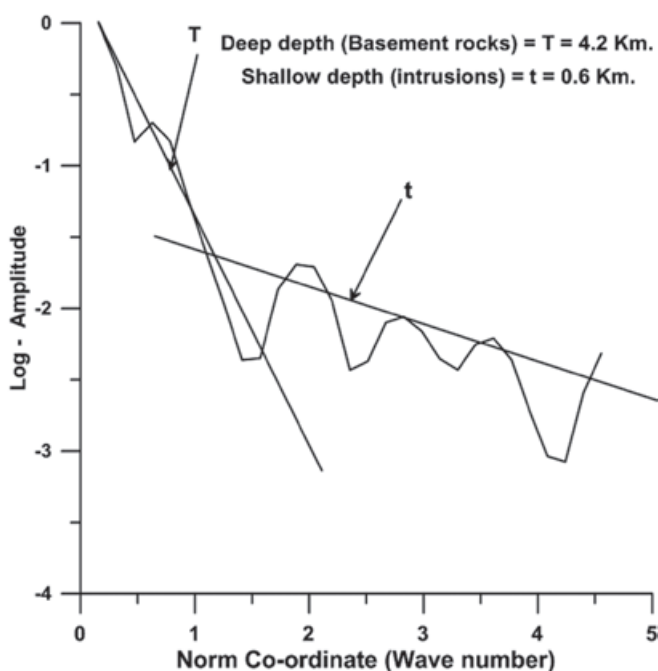


Figure 13. Spectral analysis from land magnetic map parallel to the location of seismic line (127).

The results deduced from the land magnetic data (Figure 10) are correlated with the results of the trend analysis technique due to the detailed survey contains more detailed information. Meanwhile the results of RTP aeromagnetic data (Figure 11) show less similarities with trend analysis owing to the regional survey may be poor in minor details.

Two and half dimensions model technique

The computation of the magnetic field due to 2.5-D model polygonal homogeneous magnetized bodies of arbitrary shape at a point (x, y, z) expressed by Ku (1977) is as follows:

$$A_{DIP}(x, z) \frac{2(J \cdot R)}{R^2} \quad (5)$$

where: J is the magnetization vector, R is the radial vector between the point x, y, z and a point in the volume x', y', z' and equal to:

$$R = \sqrt{(x' - x)^2 + (y' - y)^2 + (z' - z)^2} \quad (6)$$

Computations of the magnetic effects for models with complex geometry have been carried out using GM-SYS computer program, by Northwest Geophysical Associates, Inc. (1995),

for an arbitrary two-dimensional polygon (c. e., Talwani, and Ewing).

The results show that the profile A1-A1' is affected by four faults from south to north (Figure 15). Whereas profile A2-A2' shows that it is affected by one fault F4 (Figure 16). In general the configuration of the basement surface obtained from 2.5-D modelling technique illustrates that the main depth of the area increases towards the north and west directions. The main depths to the basement surface range between 3.5 and 4.5 km.

Seismic lines interpretations

Two seismic lines WQ85-31B and 127 were prepared by Egyptian General Petroleum Cooperation (EGPC) trending N-S and E-W, respectively (Figures 17 and 18). They were correlated with the vertical velocity logs to locate the exact depths to the horizons (marker beds). These lines were interpreted to establish the shallower structures in the sedimentary rocks. These lines were correlated with the profiles interpreted from 2.5-D modeling technique.

This correlation reveals that the structures interpreted from these seismic lines correlate well with features deduced from the geomagnetic interpretations along the same profiles. This correlation also indicates that these structures are extending from the subsurface basement rocks upward to the sedimentary sequences.

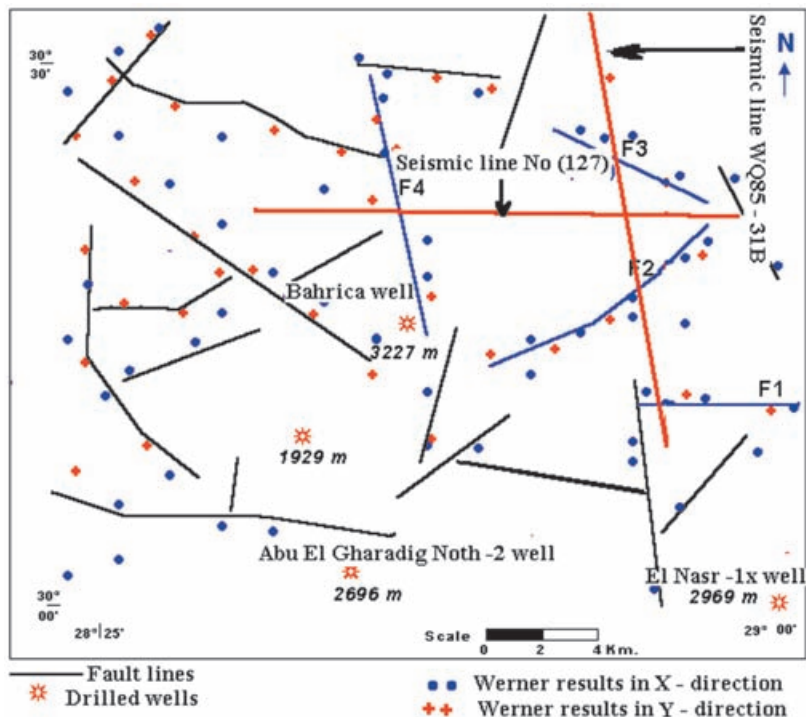


Figure 14. Result of application Werner and Euler deconvolution methods to RTP land magnetic map.

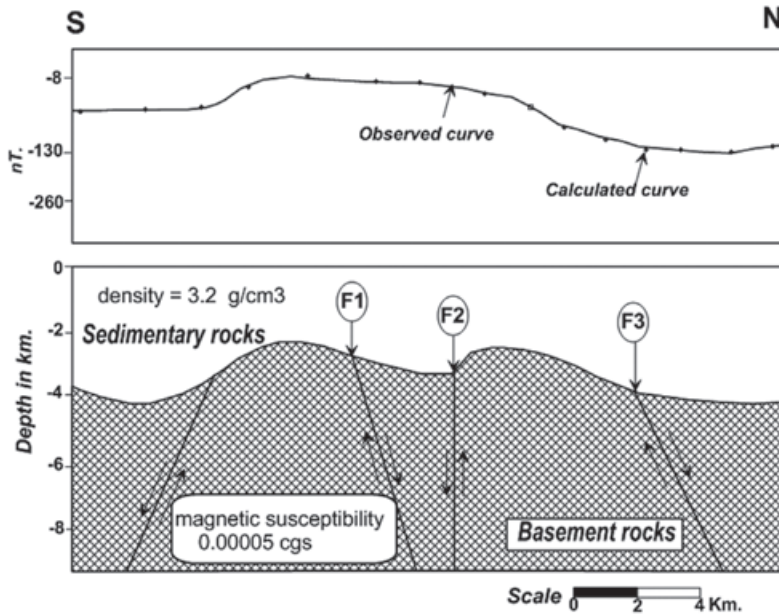


Figure 15. Two and half dimensions geomagnetic model along profile A1-A1' of the land magnetic map.

a-Interpretation along line WQ85-31B:

- The length of this line (Figure 17), is more than 18 km and covers from nearly the southern to the northern parts of the study area. The interpretation along this line indicates that there are three normal faults affecting the sedimentary section. These faults are affecting Bahariya, Abu Roash, Khoman, and Apollonia formations. The mean depth to the upper surface of these faults is about 600 meter. The deduced faults can be correlated approximately with the faults F1, F2 and F3 deduced from the interpretations of geomagnetic data.

b- Interpretation along line 127:

- This seismic line (Figure 18), extends in E-W direction and covers more than 24 km. This line is parallel to the profile L2 - L2' along the RTP land magnetic map. This line is affected by two faults. The first fault cuts Bahariya, Abu Roash, Khoman, and Apollonia formations and the other branch of this fault cuts only the Bahariya formation. The second fault passes Bahariya Fm and it is the oldest. Also, the we note that the first fault correlated with the F4 deduced by geomagnetic interpretations. The depth to the upper surface of this fault reaches about 600 m.

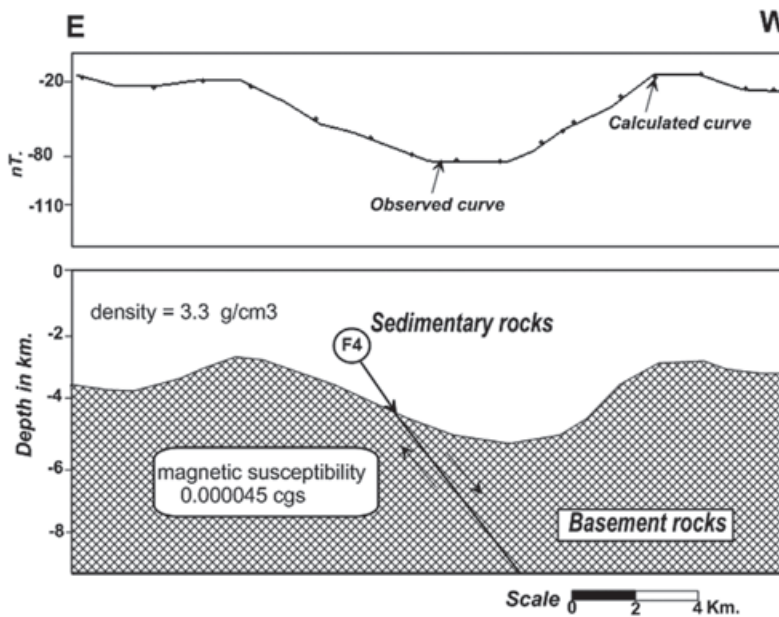


Figure 16. Two dimensions geomagnetic model along profile A2' - A2 of the land magnetic map.

Figure 17. Interpreted geoseismic structural cross-section along seismic line WQ85-51B.

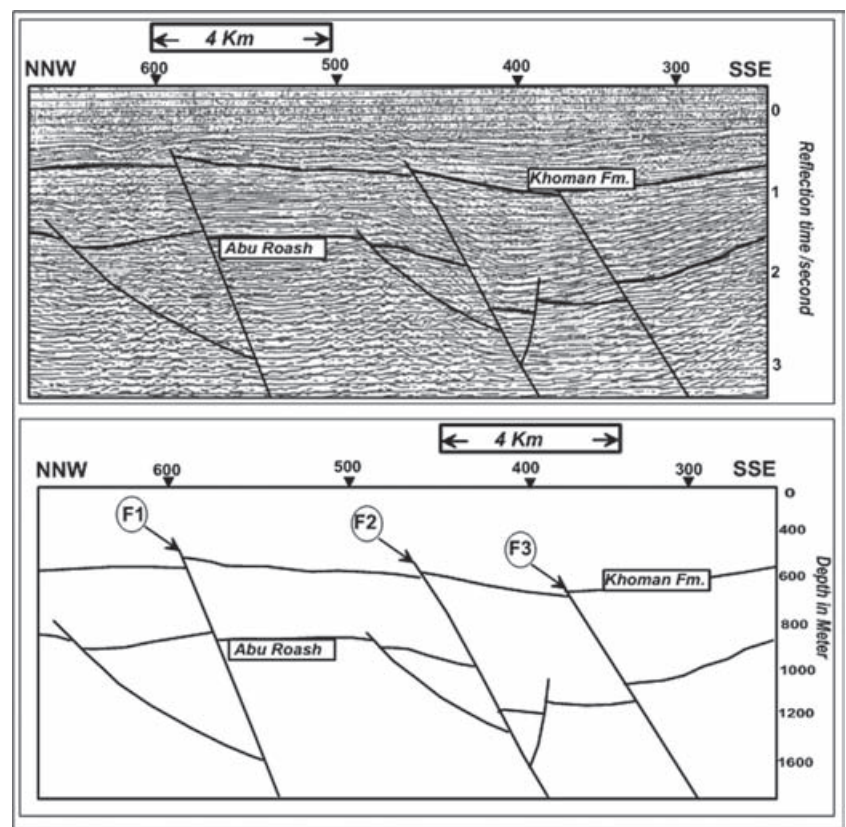
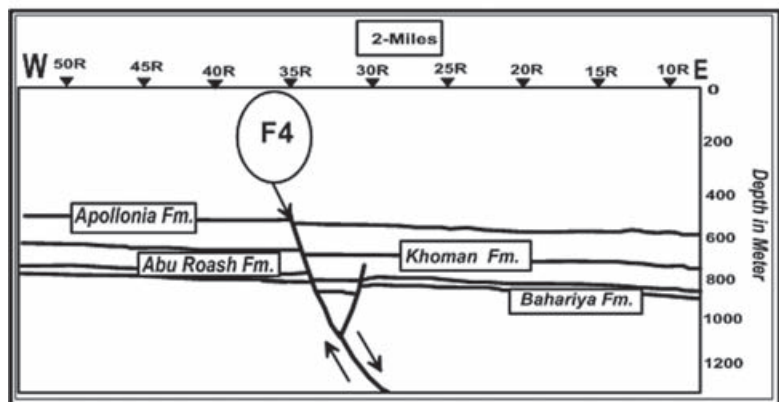
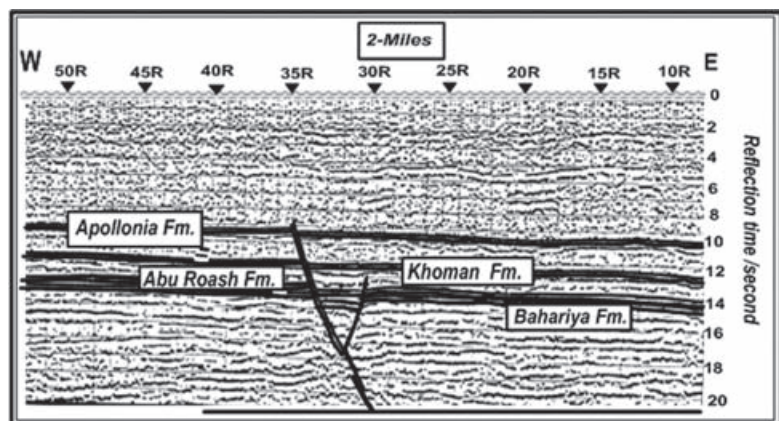


Figure 18. Interpreted geoseismic structural cross-section along seismic line No. (127).

Discussion and conclusions

In this study, a correlation carried out between the structures deduced from the geomagnetic data and the structures deduced from the seismic data. Accordingly an agreement and indicates that these structures are extending from the subsurface basement rocks upward to the sedimentary sequence. It proves the capability of the geomagnetic method to detect the structures of the basement rocks which extends to the overlying sedimentary rocks. This leads to the conclusion that the geomagnetic tool is an effective geophysical method in the fields of exploration and prospecting if we applied the suitable interpretation methods and techniques. The tectonic trends affecting the area are $N35^{\circ} - 45^{\circ} W$ parallel to the Gulf of Suez, $N45^{\circ} - 65^{\circ} E$, related to the Syrian Arc tectonics, E - W belong to the Mediterranean and Aqaba trends.

Also, these structures trends are correlated fairly well with the results deduced from Euler method and the interpreted seismic sections. The depths to the basement rocks range between 3.1 and 4.3 km, which matched with the drilled wells in the study area.

The deduced fault structures, imply that all of them do not affect Quaternary or near surface rocks. This is also indicated from seismicity map of north-western Egypt compiled by ENSN. The possible interpretation for this outcome is that the study area is recently more stable than other adjacent areas in the northern parts of Egypt.

This work provides a guide line for any exploration process, and for establish any new towns or strategic projects in the area.

Bibliography

Abdel Hady A.M., Kolkila A.A., Abdou M.F., 1988, Subsurface Aptian rocks in some parts of the North Western desert; their geologic setting and hydrocarbon potentiality, Egypt, *J. Geol.*, 32, 219-241.

Badr El Din Petroleum Co., 2004, Seismic Survey at the northeastern part of Qattara Depression, internal report, Cairo, Egypt.

Barakat M.G., 1982, General review of Petroliferous Provinces of Egypt with special emphasis on their geologic setting and oil potentialities. *Petro. and Gas. Proj.*, Cairo Univ., M. I. T., p. 86.

Baranov V., 1975, Potential field and their transformation in applied geophysics. *Geoexploration Monograph*, Series L, No. 6: Gerbruder Borntraeger, Berlin, Stuttgart, Germany.

Båth M., 1974, Spectral analysis in Geophysics. Elsevier Scientific Publ. Company, Amsterdam, New York.

Conoco and General Petroleum Corporation, 1987, Geological map of Egypt, Scale 1 : 500,000: Bernice, Cairo-Egypt.

Egyptian General Petroleum Co-operation, 1979, Aeromagnetic map Scale 1 : 100000, General Petroleum company.

GM-SYS. 1995, Gravity and magnetic modelling, version 3.6; Northwest Geophysical Association, Inc. (NGA), Corvallis, Oregon, U.S.A. 97339.

Henderson R.G., 1960, A comprehensive system of automatic computation in magnetic and gravity interpretation, *Geophys.*, 30, 569-585.

Hildenbrand T.G., 1983, Filtering program based on two dimensional Fourier analysis, A. U.S. Geological survey open-file report, 83-237, p. 31.

Khalda Petroleum Co., 2000, Seismic Survey at Abu Senna basin southern part of Qattara Depression, internal report, Cairo, Egypt.

Ku C.C., 1977, A direct computation of gravity and magnetic anomalies caused by 2- and 3-D bodies of arbitrary magnetic polarization by equivalent-point method. *Geophysics, Soc. of Expl. Geophys.*, 42, 610-622.

Ku C.C., Sharp J.A., 1983, Werner deconvolution for automated interpretation and its refinement using Marquardt's Inverse Modeling. *Geophysics*, 28, 754-774.

Nettleton L.L., 1976, Gravity and magnetic in oil prospecting. Mc-Graw- Hill Book Co, New York.

Pasteka R., 2001, Comment on the structural index used in Euler deconvolution for the step structure in gravimetry. Extended abstracts from EAGE 63rd Conference and technical exhibition, Amsterdam, p. 211.

Reid J.M., Allsop H. Granser, 1990, Magnetic interpretation in three dimensions using Euler deconvolution. *Geophysics*, 55, 80-91.

Said R., 1990, The geology of Egypt. Balkemor Publishers, Rotterdam, Netherlands, 364-380.

Talwani M., Ewing M., 1960, Rapid computation of gravitational attraction of three-dimensional bodies of arbitrary shape. *Geophysics*, 25, 203-225.

Thompson D.T., 1982, EULDPH – A new technique for making computer-assisted depth estimates from magnetic data. *Geophysics*, 47, 31 – 37.

Zurflueh E.G., 1967, Application of two dimensional linear wavelength filtering. *Geophys.* 32, 1,015 - 1,035.

Werner S., 1953, Interpretation of magnetic anomalies at sheet-like bodies, *sveriges Geol. Undersok, Ser., C., Arsbok*, 6, 413 – 449.